RATINGS OF RICE LEAF BLAST DISEASE BASED ON IMAGE PROCESSING AND STEPWISE REGRESSION

M. Xiao, Z. Deng, Y. Ma, S. Hou, S. Zhao

HIGHLIGHTS

- Multi-feature fusion of morphology and texture features
- Stepwise regression analysis to distinguish disease areas from natural brown areas
- Calculate the ratio of the total area of the diseased area to the area of the leaf area to obtain the disease level

ABSTRACT. *In this research, an evaluation method involving digital image processing and stepwise regression was studied to establish an efficient and accurate rating system for studying rice blast disease. For this purpose, the R-G image was segmented by using maximum interclass variance method in which the lesion and naturally withered region was extracted from the leaves. Then, 240 lesion areas and 240 natural yellow areas were selected as samples. During the experiment, ten morphological features and five texture features were extracted. Subsequently, for lesion identification, stepwise regression analysis, SVM and BP neural network were used. In the results, regression analysis of naturally yellow areas showed the highest accuracy in lesion identification, reaching 93.33% for disaster-level assessment of identified lesion areas. On the basis of the results, it is evident that 153 samples were correctly classified into divisions of 160 tested different rice blast leaves, with 95.63% classification accuracy. This study has introduced a new method for objective assessment of leaf blast disease.*

Keywords. *Disease classification, Lesion identification, Maximum interclass variance method, Rice blast, Stepwise regression.*

Rice blast is one of the three major diseases of rice which seriously affects rice production, causing an estimated 10% to 30% reduction in rice production and also negatively affects rice quality (Wen et al., 2013; Xiao et al., 2018). At present, the degree of rice blast in rice is identified through visual assessment. Apart from being a highly subjective form of classification, this type of identification requires high degree of expertise. Even so, the efficiency of such a method of classification is low, often resulting in deviations. There is a growing demand for quick and accurate prediction and comprehensive classification of the extent of the rice blast disease. Moreover, there is a pressing need for effective measures to control and prevent this common plant disease, opening new pathways for future researches regarding rice disease diagnosis.

Submitted for review in January 2019 as manuscript number ITSC 13131; approved for publication as a Research Article by the Information Technology, Sensors, & Control Systems Community of ASABE in September 2019.

The authors are **Maohua Xiao,** Associate Professor, **Ziang Deng,** Student, **You Ma,** Graduate Student, **Shishuang Hou,** Student, **Sanqin Zhao,** Associate Professor, Department of Mechanical Engineering, College of Engineering, Nanjing Agricultural University, Nanjing, Jiangsu, China. **Corresponding author:** Maohua Xiao, 40# Dianjiangtai Road, Pukou District, Nanjing 210031, PR China; phone: +86 139 5175 6153; e-mail: xiaomaohua@njau.edu.cn.

At present, there are a number of studies centering on rice blast disease detection pertaining to China and other countries. However, there are relatively few studies to evaluate the degree of disease and mark its early diagnosis (Wang et al., 2015). Common disease grading techniques include hyperspectral imaging techniques (Bock et al., 2010; Jin et al., 2013; Zheng et al., 2013; Xu et al., 2019b) and image processing techniques (Ge et al., 2008; Wijekoon et al., 2008; Rastogi et al., 2015). For grading disease using hyperspectral imaging technology, the procedure is outlined as follows. Firstly, images of diseased leaves are acquired utilizing hyperspectral imaging technology. Then, this image is analyzed and processed, and finally the level of disease is gauged. This method results in high accuracy for grading without natural yellow leaves, but the treatment efficiency is low. For image processing method, image of diseased region is obtained. Then, the ratio of diseased area with area of the entire leaf is obtained to calculate the extent of disease. This method yields high efficiency; however, the grading accuracy is slightly lower than the precision obtained using hyperspectral imaging methods. Although hyperspectral imaging techniques (Zheng et al., 2013; Huang et al., 2015), chlorophyll fluorescence spectrometry (Zhou et al., 2014) and image processing methods (Ma et al., 2008) have been reported for grading rice blast disease, the lack of natural yellow leaves (fig. 1) in these studies has led to disease grading. In light of the researches discussed above, this study has

Figure 1. Diseased leaves containing natural yellow areas.

proposed a method for grading leaf blast disease utilizing image processing and stepwise regression.

For methodology, image for diseased region was obtained using camera and this image was then preprocessed. Subsequently, morphology and texture features of diseased part were extracted. In the final step, the stepwise regression model was established to extract the disease area. By calculating the lesion area and the percentage of leaf area, extent of the disease was calculated. The classification accuracy rate obtained reached 95.63% in the case of the interference of dry naturally yellow leaves.

MATERIALS AND METHODS

The sample images used in this research have been acquired from the rice experimental field of Jiangpu farm at Nanjing Agricultural University. Most of the rice blast lesions in paddy field are found to be round or elliptical, their colors are dark green and brown which denote typical chronic rice blast and brown-spot type rice blast (Liu et al., 2014).

For sample collection, experimental device was established near the rice field, and the camera is placed 0.3 m above the sample. Under natural light, Zenmuse Z3 camera from Da Jiang Innovate Technology Ltd, (Nanjing, China) (resolution 4000 × 3000) with single focal-length mode was used to shoot rice leaves. To eliminate images of background, an A4 paper was placed under the leaves before shooting. In this experiment, a total of 270 leaf samples with different degrees of disease were captured; out of these 258 images were valid. As images for samples were captured in natural light, on sunny days the sampling was conducted from 7:00 A.M. to 10:00 A.M. or from 4:00 P.M. to 6:00 P.M. At other times, sampling was conducted with corresponding shading measures. On cloudy days, sampling was carried out throughout the day. Figure 2 shows the leaves of rice blast with different disease levels.

The obtained disease sample images were imported in the computer in.JPG format. In order to calculate the relatively large blade aspect ratio, the sample images were cropped to fit the entire screen, thus reducing the time required used for image processing. The size of the image processed in the experiment was 2500 × 200 pixels, and image processing algorithm was implemented in MATLAB (MathWorks, 2014b).

DATA PREPROCESSING AND FEATURE EXTRACTION

IMAGE SMOOTHING

Rice blast samples were photographed in natural light. These samples were then artificially manipulated and preserved. This in turn affected noise and subsequent feature extraction, so the images were smoothed first, and then the lesion sites were split. Before conducting image filtering, gray image processing and histogram equalization was operated to enhance the image effect (Lu et al., 2011). In order to remove the noise and to enhance the image edges and textures, the median filter for smoothing was selected and the filter window size was specified at 3 × 3 pixels.

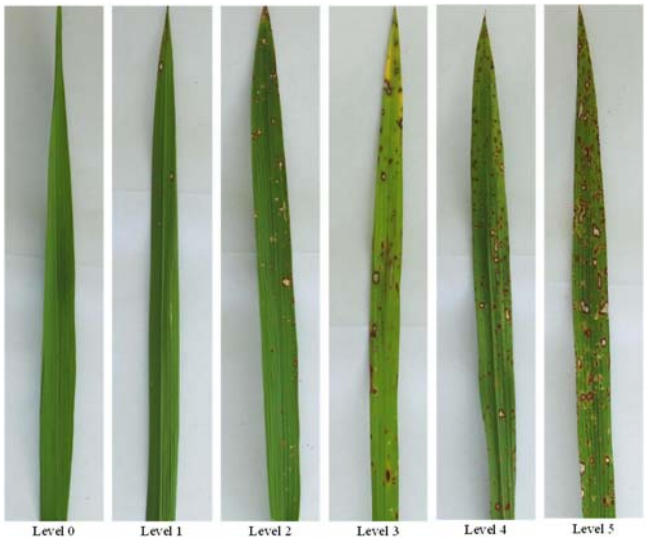

Figure 2. Rice blast image.

IMAGE SEGMENTATION

Image segmentation is a technique and process used for dividing the image into distinct regions and extraction of region of interest (ROI). In this study, segmentation was performed twice to gain the area of leaves and lesions.

The Segmentation of Leaves and Background

Because the background of the sample images was white, and there was a striking difference between gray value of the leaf and the background, a bimodal characteristic appeared in the histogram due to which the left side of the peak overlapped with the area of leaves with low gray value. Despite image smoothing, appearance of some cracks in the peak of background area were inevitable due to uneven illumination caused by natural light; though these did not affect the segmentation. By analyzing the distribution of red, green and blue channels in samples acquired at different times, the bimodal difference of blue component histogram was found to be the greatest, hence, the blue channel was used to divide leaves and background. The segmentation effect is shown in figure 3, and the calculation formula used for segmentation (Tang et al., 2015) is shown in equation 1.

(a) The diagram of blue component.

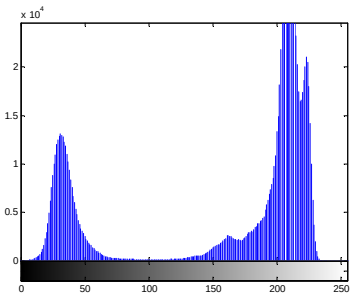

(b) Blue component histogram

(c) The binary image of leaf area

Figure 3. The segmentation of leaf area.

$$g(x,y)=\begin{cases}255 & f(x,y)\geq T\\ 0 & f(x,y)<T\end{cases} \quad (1)$$

In the formula, $f(x, y)$ denotes the pixel value of blue channel image, $g(x, y)$ is the pixel value of the image after binarization processing, and T is the gray value of the trough in the histogram, T = 100 in this study.

The Segmentation of Yellow Areas and Leaves

As gray value of yellow and natural site were different, hence Threshold segmentation method was used to divide the yellow site and normal site. To avoid the subjectivity of artificially choosing the threshold, we chose a global automatic threshold selection method: maximum interclass variance method (Wan and Duan, 2008). The maximum interclass variance method performs image segmentation according to the principle of maximum variance. The larger the variance between the background and the target, the greater the difference between the two parts that make up the image. When part of the target is divided into the background or part of the background is divided into the target, the difference between the two parts will be smaller.

In the experiment, the RGB component histogram was analyzed, and the G-B, R-G, and 2G-R-B images were transformed into binary images by using the maximum interclass variance method. A bitwise AND was performed on binarization graph and original images to obtain superimposed effect map, the process is shown in figure 4.

In this regard, R-G image segmentation effect was found to be the most significant, as illustrated in figure 5. Therefore, R-G component combination was ultimately selected for processing.

Figure 4. The segmentation of disease area.

(a) The original image of sample.

(b) The binary image of sample.

(c) The superimposed effect image.

Figure 5. Segmenting lesions image by using maximum interclass variance method.

MORPHOLOGICAL OPERATIONS

The binary image obtained after processing had lost some aspects of detailed information as compared to the original image. Morphological processing can effectively eliminate some of the isolated dots present in the image. Additionally, it can fill holes, smooth out the edges, and effectively reduce interference of small points in the analysis (Wu et al., 2017). In this study, 2×2 disc structure elements were used to perform open operation and for eliminating small points. Then, 3×3 disc structure elements were used to perform close operation for filling the dilatation erosion. The morphological processing is shown in figure 6.

FEATURE EXTRACTION

Image feature extraction needs to be carried out after obtaining image segmentation, color feature, texture feature and morphological features as common image features (Ruiz et al., 2011). It was observed that the lesions had similarity in their color to naturally yellow areas, but there are some differences in their morphology and texture. Thus, these lesions could be partially extracted on the basis of their morphological and textural features.

Morphological Feature Extraction

This research study extracted 10 morphological features of lesions: area (the number of pixels present in a lesion area), eccentricity (eccentricity of an ellipse with the same standard second-order central moment as the region), minimum circumscribed rectangle area (in the pixel sense), perimeter (the number of contour pixels in lesion area), long axis, short axis, ovality, rectangularity, ratio of long axis to short axis of the equivalent ellipse, and complexity. Among these features, ovality, rectangularity, and complexity were calculated by using the formula listed in equations 2-4.

Ovality: $$E=\frac{a-b}{a} \quad (2)$$

Rectangularity: $$R_{sq}=\frac{A}{SMER} \quad (3)$$

Complexity: $$C=\frac{P^2}{A} \quad (4)$$

Figure 6. Morphological processing image.

In equations 2-4, a and b denote the major and minor axis lengths of the ellipse equivalent to the lesion area in the pixel sense, respectively. Also, A represents the lesion area, P is the circumference, and SMER is the smallest circumscribed rectangle area.

Texture Feature Extraction

Texture features serve as important indicators to distinguish between the diseased spots and naturally yellow leaves. At the same time, the co-occurrence of gray with the rest of the image reflected the main texture features of the image. Following specifications were made: $f(x, y)$ was set as a two-dimensional digital image, image size was selected as $M \times N$, and gray level as L. Assuming that (x_1, y_1) and (x_2, y_2) are two pixels in $f(x, y)$, the distance is denoted by d and the angle between two pixels and the ordinate is θ. Hence, the gray level co-occurrence matrix $P(i, j \mid d, \theta)$ is obtained (Tang et al., 2008) as:

$$P(i,j \mid d,\theta) = \#\{(x_1,y_1),(x_2,y_2) \in M \times N \mid d,\theta, f(x_1,y_1) = i, f(x_2,y_2) = j\} \quad (5)$$

where # {x} represents the number of cells in the curly brackets, θ represents the span value, and the interval is generally limited to 45°.

In this study, five parameters including entropy (ENT), angular second moment (ASM), contrast (CON), correlation (COR), and inverse difference moment (IDM) were selected as the texture features to ascertain lesion recognition. An explanation of the five parameters can be found in the Parekh and Bhattacharya (2015)

LESIONS RECOGNITION

STEPWISE REGRESSION ANALYSIS

The basic idea behind using stepwise regression is to incorporate the characteristic parameters of lesions into the model one by one. This process includes the following sequence: first, by F test (Xu et al., 2019a) is carried out on each parameter after introduction. Then, if the original variable demonstrates no significant function any longer after the introduction of the variable, then the variable is deleted. This way, only significant variables are included in the regression equation before each the introduction of each new variable (Si and Sun, 2015).

The correlation analysis was carried out on the extracted feature data by using regression analysis. Each parameter of every feature was set as a dependent variable, and other feature parameters were then set as independent variables in order to analyze the correlation between features. The correlation results are illustrated in figure 7.

It is evident from the Fig that the eccentricity of the lesion is highly correlated with other features; however, the shape of the naturally yellow leaves is irregular. Therefore, the eccentricity was used as the parameter in this research to distinguish lesions from natural yellow leaves. For this purpose, 120 lesions were selected, and three regression equations with eccentricity (e) were established, as shown in table 1. It

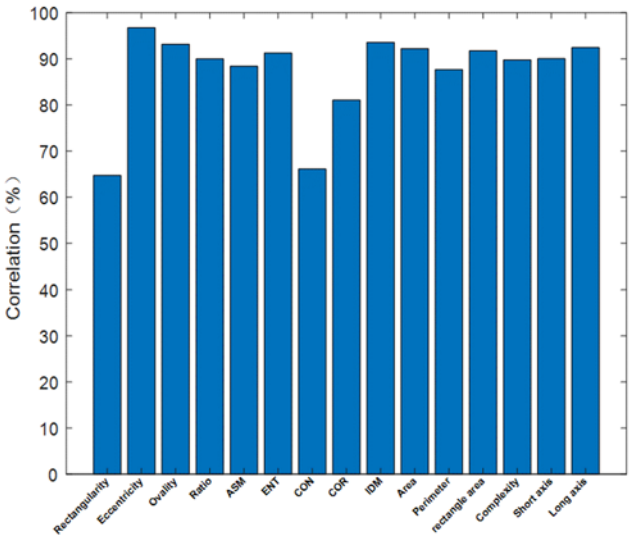

Figure 7. Correlation analysis diagram.

can be seen from table 1 that three parameters which have the greatest influence on eccentricity are ellipticity, complexity, and rectangularity. The coefficient of determination of eccentricity was calculated as R^2=0.932.

In order to extract the morphological parameters of all lesions and naturally yellow areas on rice leaves, regional markers were needed. The area mark is the same as the pixels connected components, and the different connection components were attached using different markings (Jia and Ji, 2013). By using regional markers, different markers could be attached on the lesions and naturally yellow areas in order to calculate the characteristic parameters of shape in the foreground area. In this study, the eight-neighborhood labeling was used to identify the foreground target, and 240 characteristic parameters of yellow areas were identified through observation.

The data obtained for 120 lesions and 120 natural yellow leaves was substituted into the established regression equation to obtain the predicted value of eccentricity. It was found that | predicted value – actual value| of lesions areas <0.08 accounted for 93.33%, while the | predicted value – actual value| of naturally yellow areas <0.08 accounted for less than 6% of the total region, At the same time, in this study, Support Vector Machines (SVM) (Hearst et al., 1998) and back propagation neural network (BP) (Jin et al., 2000) methods were used to extract lesions. SVM and BP neural network specified 120 lesions and 120 natural yellow leaves to encompass the training set, and 120 lesions and 120 natural yellow leaves as test sets. The classification accuracy rate of SVM under different kernel functions is shown in table 2.

When using BP neural network classification, the classification accuracy rate of different hidden layers is tested. In

Table 1. Eccentricity regression analysis equation.[a]

Stepwise Regression Equation
e=0.444+0.771*E(R^2=0.804 P<0.0001)
e=0.476+0.928*E-0.0075*C(R^2=0.862 P<0.0001)
e=0.488+0.925*E-0.0074*C-0.0154*Rsq (R^2=0.932 P<0.0001)

[a] e: eccentricity; E: ellipticity; C: complexity; Rsq: rectangularity4.2 Lesions extraction.

Table 2. Different nuclear function classification accuracy.[a]

Sample	Kernel Function		
	Linear	Polynomial	RBF
Lesion area	84.17%	85.83%	91.67%
Natural yellow leaf area	83.33%	82.5%	86.67%

[a] The parameters under the best classification accuracy of the RBF kernel are set to c=0.1, g=1.

this study, 15 feature vectors are obtained by the feature extraction module. These feature vectors are input into the BP neural network as parameters, so the input layer is set to 15. Since it is a two-class problem, the output layer is set to 2. Since the input layer and the output layer are fixed, it is only necessary to discuss the influence of the hidden layer number on the network classification effect. Figure 8 describes the classification accuracy of BP network under different hidden layer numbers. It can be seen from figure 8 that the number of hidden layers is 10 when the accuracy is the highest, so the optimal classification structure of BP network in the research process is 15-10-2.

The test results attained for the three methods are shown in table 3. It is clear from table 3 that in the case of natural yellow leaves, the stepwise regression analysis of the three algorithms shows the highest rate of correct recognition of lesions, reaching 93.33% accuracy, and the false positive rate for natural yellow leaves is found to be the lowest. Therefore, stepwise regression analysis was used in this study for lesion extraction. It was considered that when the foreground target |predicted value-actual value| less than 0.08, the region was regarded as a lesion. The actual value is the eccentricity (eccentricity rate) obtained by the feature extraction module. The eccentricity of different lesions or natural yellow leaves is different, and the actual value is not a fixed value. For foreground targets that did not meet the above-mentioned criteria, their pixel values were set to the background color (as shown in fig. 9).

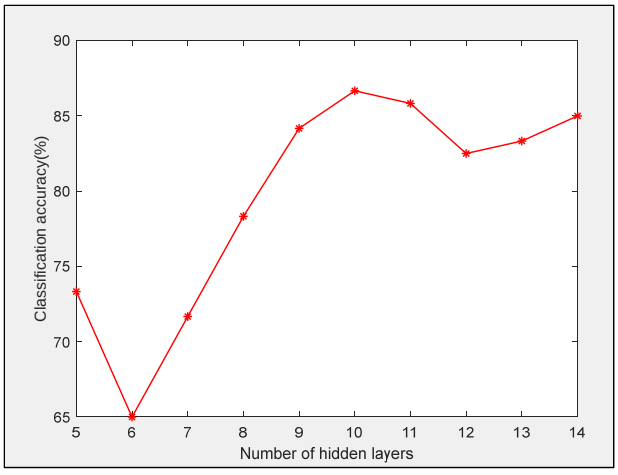

Figure 8. Different hidden layer classification accuracy.

(a) The image of sample binarization.

(b) The binary image only with lesions.

Figure 9. Extracting the lesion map by stepwise regression method.

CLASSIFICATION OF DISEASE DEGREE

In this study, the criteria for grading the extent of rice blast disease has been based on the actual operation standard and the national standards for rice blast. Thus, rice leaf blast cases were classified into 6 grades based on that criteria. The leaves were then classified according to the percentage of leaf area.

$$S = \frac{A_2}{A_1} \tag{6}$$

In the equation, S is the lesion area percentage of leaf area, A_1 represents the leaf area (in pixel sense), and A_2 denotes the lesion area (in pixels). The flow chart for classifying lesions is illustrated in the following figure 10.

A total of 258 valid samples with different grades of disease were collected; out of these 160 samples were selected for testing. The sample images were then imported into CAD. Then, the ratio of lesion area to the leaf area was manually measured, with each picture measured a total of three times, and finally mean was calculated for the resultant value

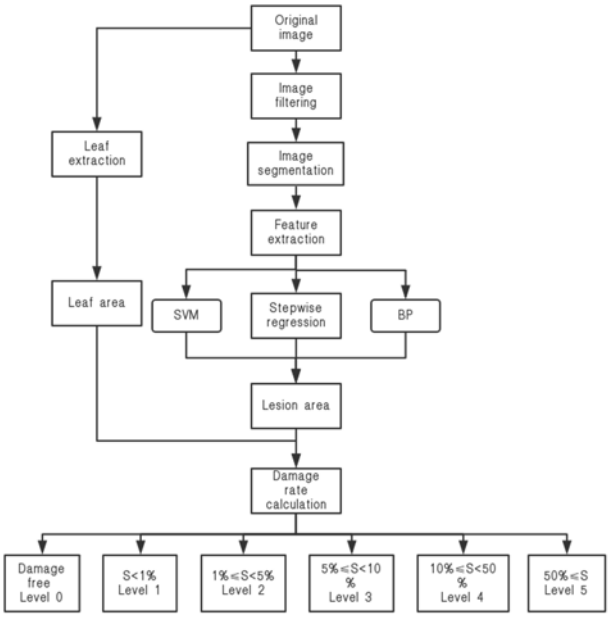

Figure 10. The flow chart of classifying disease degree.

Table 3. Three algorithms under natural yellow leaves accurately identify the lesions.

Method	Sample		Accurate Recognition of Lesions	Accurate Recognition Rate of Lesions (%)	Natural Yellow Leaf False Recognition	Natural Yellow Leaf False Recognition Rate (%)
	Number of Lesions	Natural Yellow Leaves				
Regression analysis	120	120	112	93.33	7	5.83
SVM	120	120	110	91.67	16	13.33
BP	120	120	104	86.67	23	19.17

Table 4. The accuracy table of disease grade.

Grade	Number of Samples	Number of Errors	Accuracy (%)
0	22	0	100
1	44	2	95.45
2	21	2	90.47
3	25	1	96
4	30	0	100
5	18	2	88.89
0~5	160	7	95.63

as the standard to reduce measurement error. Through testing the samples through both image processing and stepwise regression methods, following accuracy rate was obtained as shown in table 4. The error quantity is derived based on manual measurement results. If the method measured by the paper is different from the manual measurement result, it is considered to be an error.

Factors affecting the classification of samples include: (1) a small number of infected lesions that were not yellow and resulted in poor segmentation effect (2) disease samples obtained in the two-level classification of critical point which easily lead to classification errors.

Additionally, this study analyzed the correlation between damage rate (measured value and predicted value) for 0-5 test samples. The correlation between the artificially obtained disease level (actual value) and the algorithm's disease level (predicted value) is mainly to evaluate the effect of the paper algorithm. The distribution of damage rate is shown in figure 11. Measured coefficient of the measured value and predicted value was calculated as R^2=0.963. As can be seen from figure 11, it can be seen that the measured value and the predicted value of the disease rate have a good fitting degree and can be used for the prediction of the test result within the error tolerance range, that is, the disease level of the rice blast can be evaluated according to the algorithm proposed in this article.

DISCUSSION

For lesions and naturally yellow areas, the morphological and texture parameters were extracted, and stepwise regression analysis equations, SVM, and BP neural network recognition models were established. The stepwise regression analysis classification result is an interval fluctuation value: | predicted value - test value | < 0.08 are lesion areas. The lesion classification is inclusive. Because some lesion areas have certain irregularities, the classification of SVM and BP training models will cause misjudgment, however, the interval fluctuation performance of stepwise regression will accommodate this slight irregularity change.

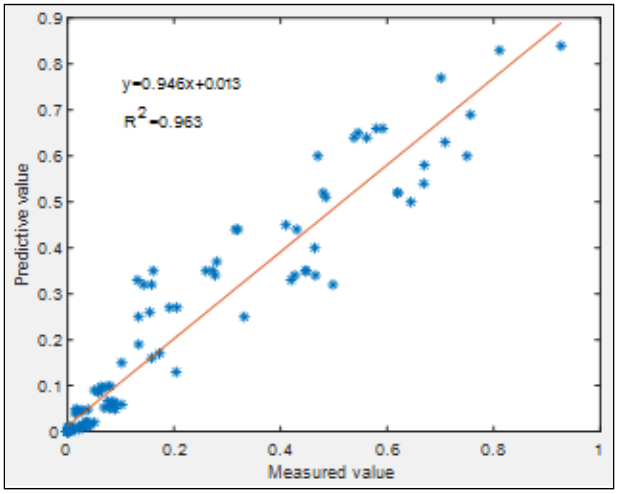

Figure 11. Fitting image of predicted and measured values of victimization rate.

At present, there are few reports on the classification of rice blast disease. The existing grading literatures are listed in the table 5. It can be seen from the table that the existing research mainly focuses on hyperspectral and fluorescence spectrum images and few of them directly process color images. In this study, rice blast classification was classified in RGB images, and the classification accuracy rate is 95.63%. The accuracy is higher than that of Ma et al. (2008) which is 90%. Because of the study of Ma et al. (2008), only the longest axis of the largest lesion was used to evaluate the grade of rice blast. Compared with single feature evaluation, multi-feature fusion evaluation was better. It is also higher than the accuracy of Zhou et al. (2014) in the classification of fluorescence spectrum images and the accuracy of Huang et al. (2015) in the classification of hyperspectral images which are 91.7% and 81.43%, respectively. In addition, the classification result of Zheng et al. (2013) is 96.39%, which is better than the research results. The reason is summarized as (i) natural yellow leaf interference is avoided during the research process. (ii) Hyperspectral images used in studies such as Zheng et al. (2013) and the interference factors during the shooting were not as much as natural light. However, hyperspectral image studies in real environments are rarely commercialized, mainly because of slow processing speeds and high costs. In summary, the method proposed in this study has certain research value.

CONCLUSION

In this research article, image processing and stepwise regression analysis were used to select a method for classifying rice leaf blast disease. As a result of this evaluation, following conclusions were drawn:

(1) Based on the color component histogram obtained for rice leaf blast samples in which $R-G$ component combination was used to divide the lesion and the leaf, the segmentation effect was obvious, allowing to effectively overcome unfavorable factors such as natural light. This algorithm proved to be useful, simple and allowed direct processing of the sample.

(2) The morphological and texture parameters of lesions and naturally yellow areas were extracted. For extracting lesions, stepwise regression analysis, SVM

Table 5. Rice blast classification literature.

Sources	Accuracy (%)	Type of Images
Zheng et al. (2013)	96.39	Hyperspectral image
Huang et al. (2015)	81.41	Hyperspectral image
Zhou et al. (2014)	91.7	Fluorescence spectroscopy
Ma et al. (2008)	90	Color image
This research	95.63	Color image

and BP neural network methods were used. The obtained results show that stepwise regression method has the highest rate of disease spot recognition and also lowest false recognition rate for natural yellow leaves under the condition of |predicted value-actual value| <0.08.

(3) The experimental results illustrate that 153 out of 160 test samples have been accurately diagnosed with the accuracy rate at 95.63%. Hence, the used method can effectively evaluate the disease level of rice blast disease quickly and accurately. Moreover, it provides new research ideas for evaluation of the degree of rice leaf blast disease in the fields.

ACKNOWLEDGEMENTS

The research is funded by National Natural Science Foundation of China (30771244) and Program for Student Innovation through Research and Training of Nanjing Agricultural University (20181037087).

REFERENCES

Bock, C. H., Poole, G. H., Parker, P. E., & Gottwald, T. R. (2010). Plant disease severity estimated visually, by digital photography and image analysis, and by hyperspectral imaging. *Critical Rev. Plant Sci., 29*(2), 59-107. https://doi.org/10.1080/07352681003617285

Ge, J., Shao, L. S., Ding, K. J., Li, J., & Zhao, S. Y. (2008). Image detecting for hazard levels of corn spots. *CSAM*, 114-117.

Hearst, M. A., Dumais, S. T., Osuna, E., Platt, J., & Scholkopf, B. (1998). Support vector machines. *IEEE Intelligent Syst. Appl., 13*(4), 18-28. https://doi.org/10.1109/5254.708428

Huang, S., Qi, L., Ma, X., Xue, K., Wang, W., & Zhu, X. (2015). Hyperspectral image analysis based on BoSW model for rice panicle blast grading. *Comput. Electron. Agric., 118*, 167-178. https://doi.org/10.1016/j.compag.2015.08.031

Jia, J. N., & Ji, H. Y. (2013). Recognition for cucumber disease based on leaf spot shape and neural network. *Trans. CSAE, 29*, 115-121.

Jin, N., Huang, W., Ren, Y., Luo, J., Wu, Y., Jing, Y., & Wang, D. (2013). Hyperspectral identification of cotton verticillium disease severity. *Optik, 124*(16), 2569-2573. https://doi.org/10.1016/j.ijleo.2012.07.026

Jin, W., Li, Z. J., Wei, L. S., & Zhen, H. (2000). The improvements of BP neural network learning algorithm. *Proc. 5th Int. Conf. on Signal Processing. 3*, pp. 1647-1649. IEEE.

Liu, T., Zhong, X., Sun, C., Guo, W., Chen, Y., & Sun, J. (2014). Recognition of rice leaf diseases based on computer vision. *Scientia Agricultura Sinica, 47*(4), 664-674.

Lu, Y., Zhang, Q. N., Xu, S. X., & Liu, D. F. (2011). Study on image pre-processing for rice blast disease identification. *J. Heilongjiang Bayi Agric. University, 23*, 64-67.

Ma, D. G., Shao, L. S., Ge, J., Ding, K. J., & Qian, L. C. (2008). Detection of the harm degree of rice blast and rice sheath blight. *Chinese Agric. Sci. Bull., 24*(9), 485-489.

Parekh, R., & Bhattacharya, S. (2015). Plant leaf recognition using texture and shape features with neural classifiers. *Pattern Recognit. Lett., 58*, 61-68. https://doi.org/10.1016/j.patrec.2015.02.010

Rastogi, A., Arora, R., & Sharma, S. (2015). Leaf disease detection and grading using computer vision technology & fuzzy logic. *Proc. 2nd Int. Conf. on Signal Processing and Integrated Networks (SPIN)* (pp. 500-505). IEEE. https://doi.org/10.1109/SPIN.2015.7095350

Ruiz, L. A., Recio, J. A., Fernandez-Sarria, A., & Hermosilla, T. (2011). A feature extraction software tool for agricultural object-based image analysis. *Comput. Electron. Agric., 76*(2), 284-296. https://doi.org/10.1016/j.compag.2011.02.007

Si, S. K., & Sun, X. J. (2015). *Mathematical modeling* (pp. 406-407). Beijing, China: National Defense Industry Press.

Tang, J. T., Hu, D. Z., & Gong, M. (2008). Research on the classification of SVM-based image texture features. *Comput. Eng. Sci., 30*(8), 44-48.

Tang, Z., Su, Y. C., & Meng, J. (2015). A local binary pattern based texture descriptors for classification of tea leaves. *Neurocomput., 168*, 1011-1023. https://doi.org/10.1016/j.neucom.2015.05.024

Wang, H. C., Gao, X., Chen, T. Y., & Chen, Z. (2015). Research progress and prospect of spectral and machine vision technology on crop disease detection. *J. Agric. Mech. Res., 37*, 1-7, 12.

Wang, L., & Duan, H. C. (2008). Application of Otsu' method in multi-threshold image segmentation. *Comput. Eng. Design, 29*, 2944-2972.

Wen, X. H., Xie, M. J., Jiang, J., Yang, B. L., Shao, Y. L., He,... Zhao, Y. (2013). Advances in research on control method of rice blast. *Chinese Agric. Sci. Bull., 29*, 190-195.

Wijekoon, C. P., Goodwin, P. H., & Hsiang, T. (2008). Quantifying fungal infection of plant leaves by digital image analysis using Scion Image software. *J. Microbiol. Methods, 74*(2), 94-101. https://doi.org/10.1016/j.mimet.2008.03.008

Wu, Z. M., Cao, C. M., Xie, C. J., Wu, J. S., Hu, W. Y., & Wang, T. Y. (2017). Grading of machine picked tea based on image processing technology and neural network. *J. Tea Sci., 37*( ), 182-190.

Xiao, M. H., Ma, Y., Feng, Z. X., Deng, Z. A., Hou, S. S., Shu, L., & Lu, Z. X. (2018). Rice blast recognition based on principal component analysis and neural network. *Comput. Electron. Agric., 154*, 482-490. https://doi.org/10.1016/j.compag.2018.08.028

Xu, X. M., Chen, D., Zhang, L., & Chen, N. (2019a). Hopf bifurcation characteristics of the vehicle with rear axle compliance steering. *Shock Vibration*, (1), 1-12. https://doi.org/10.1155/2019/3402084

Xu, X., Zhang, L., Jiang, Y. P., & Chen, N. (2019b). Active control on path following and lateral stability for truck-trailer combinations. *Arabian J. Sci. Eng., 44*(2), 1365-1377. https://doi.org/10.1007/s13369-018-3527-1

Zheng, Z. X., Qi, L., Ma, X., Zhu, X. Y., & Wang, W. J. (2013). Grading method of rice leaf blast using hyperspectral imaging technology. *Trans. CSAE, 29*(19), 138-144.

Zhou, L. N., Yu, H. Y., Zhang, L., Ren, S., Sui, Y. Y., & Yu, L. J. (2014). Rice blast prediction model based on analysis of chlorophyll fluorescence spectrum. *Spectroscopy Spectral Analysis, 34*(4), 1003-1006.